



Limit analysis of strain-hardening viscoplastic cylinders under internal pressure by using the velocity control: Analytical and numerical investigation

S.-Y. Leu*

Department of Aviation Mechanical Engineering, China Institute of Technology, No. 200, Jhonghua Street, Hengshan Township, Hsinchu County 312, Taiwan, ROC

ARTICLE INFO

Article history:

Received 18 March 2008

Accepted 20 October 2008

Available online 1 November 2008

Keywords:

Limit analysis

Sequential limit analysis

Fixed point iteration

Nonlinear isotropic hardening

Viscoplasticity

Thick-walled hollow cylinder

ABSTRACT

The paper aims to assess plastic limit loads of thick-walled hollow cylinders of strain-hardening viscoplastic materials under internal pressure. Particularly, the problem concerned features in the interaction between strengthening and weakening behavior during the deformation process. Therefore, the relating onset of instability and the stability condition also deserve to be further investigated. Analytical and finite-element limit analysis efforts are both made for complete and comparative investigation. By the concept of sequential limit analysis, the plastic limit loads were acquired by solving a sequence of limit analysis problems via computational optimization techniques. Applying the velocity control as a computational strategy to simulate the action of pressure, the paper investigates analytically and numerically the plastic limit load, the onset of instability and the stability condition of plane-strain circular cylinders. Especially, analytical solutions of the onset of instability were solved explicitly by the fixed point iteration. Validation of the present analytical and finite-element efforts was made completely with good agreement between the analytical solutions and the numerical results.

© 2008 Elsevier Ltd. All rights reserved.

1. Introduction

Plastic limit load of cylinders is useful information requested frequently for an optimal structural design. As it is well known, limit analysis is a direct method to capture the asymptotic behavior of an elastic–plastic material by the lower bound or the upper bound theorem. Moreover, finite-element limit analysis [e.g. 1–15] further enhance the accuracy of limit analysis and broaden its applicability to more complex problems in engineering applications by taking advantage of techniques of finite-element methods [16] and mathematical programming [17]. On the other hand, if we consider structures made of strain-hardening viscoplastic materials, it is appropriate to evaluate the load-bearing capacity by limit analysis sequentially to illustrate the interesting interaction between strengthening and weakening behavior during the deformation process. By sequential limit analysis, it is to conduct a sequence of limit analysis problems with updating local yield criteria in addition to the configuration of the deforming structures. In each step and therefore the whole deforming process, rigorous upper bound or lower bound solutions are acquired sequentially to approach the real limit solutions. Accordingly, efforts [18–30] have illustrated

extensively that sequential limit analysis is an accurate and efficient tool for the large deformation analysis.

In this paper, we consider the limit analysis problem of a plane-strain cylinder under internal pressure. The thick-walled cylinder considered is made of strain-hardening viscoplastic materials. Thus, it is not only a typical limit analysis problem aimed to seek the plastic limit loads sequentially, but it is also an interesting problem involving the interaction of strengthening and weakening behavior reflecting the properties of the strain-hardening and the strain-rate sensitivity during the deformation process. The strengthening behavior is due to from the material hardening properties. And the weakening phenomenon is corresponding to the strain-rate sensitivity and the widening deformation of a pressurized cylinder. Thus, it also deserves to pay attention to the onset of instability and the stability condition of the plastic limit load. Note that, the onset of instability concerned is about the plastic instability marked by the limit load maximum while dealing with thick-walled cylinders [31,32]. Namely, the strengthening due to material hardening is exceeded by the weakening resulting from the strain-rate sensitivity and the widening deformation. On the other hand, it is well known in the elastic–plastic numerical analysis that the action of internal pressure can be simulated either by using the stress (or load) control or by using the velocity (or displacement) control. Identified by the simulation method of the action of pressure load, two different normalization conditions were adopted in the computational procedures of finite-element limit analysis

* Tel.: +886 3 5935707; fax: +886 3 5936297.

E-mail address: syleu@cc.chit.edu.tw

Nomenclature

a_0	initial interior radius	t	transposition superscript
a	current interior radius	Δt	step size
\dot{a}	current velocity of the interior radius	Δt_i	step size in the i th iteration
b_0	initial exterior radius	$\{U\}$	nodal-point velocity vector
b	current exterior radius	$\{U\}_0$	arbitrarily starting value of nodal-point velocity vector
$\{C\}$	coefficient matrix relating to the incompressibility constraint	$\{U\}_{j+1}$	unknown nodal-point velocity vector in the $(i+1)$ th iteration
D	problem domain	$\{U^*\}_j$	nodal-point velocity vector calculated in the i th iteration
∂D_s	static boundary	\bar{u}	velocity field
∂D_k	kinematic boundary	\bar{u}_s	velocity field prescribed at the static boundary
E_U	convergence tolerance	$\ \cdot\ _2$	Euclidean norm
G	a constant relating to the velocity control	$\ \sigma\ _\nu$	von Mises primal norm on stress tensor
h	hardening exponent	$\ \dot{\epsilon}\ _{-\nu}$	von Mises dual norm on strain-rate tensor
$[K]$	assembled stiffness matrix	σ	stress tensor
$[K_{e1}]$	element stiffness matrix	σ_r	stress component in the radial direction
$[K_{e2}]$	element stiffness matrix	σ_Y	yield strength
m	strain-rate sensitivity	$(\sigma_Y)_{j+1}^n$	yield strength updated in the $(i+1)$ th iteration of the n th step
\bar{n}	unit outward normal vector of a boundary	σ_0	initial yield strength
N_e	number of elements used to discretize the domain	σ_∞	saturation value of yield strength
$p(\{U\})$	discretized inner product of the incompressibility constraint	$\bar{\sigma}$	equivalent stress
P_i	internal pressure	$\bar{\epsilon}$	equivalent strain
q	load factor	$\bar{\epsilon}^1$	equivalent strain for the first step
$q(\sigma)$	lower bound functional	$\bar{\epsilon}^n$	equivalent strain for the n th step
$\bar{q}(\bar{u})$	upper bound functional	$\dot{\epsilon}$	strain-rate tensor
q^*	exact limit load	$\dot{\bar{\epsilon}}$	equivalent strain rate
$\bar{q}(\{U\})$	finite-element discretized upper bound functional	$\dot{\bar{\epsilon}}_0$	reference strain rate
$\bar{q}(\{U^*\}_j)$	finite-element discretized upper bound functional calculated in the i th iteration	$\dot{\bar{\epsilon}}_{j+1}^n$	equivalent strain rate updated in the $(i+1)$ th iteration of the n th step
R	yield strength ratio	δ	small real number
\bar{S}	length of the innermost edge	∇	vector differential operator
\bar{t}	scalable distribution of a traction vector	β	penalty parameter

[20–30]. In the stress control approach, the normalization condition is based on the simulation of the action of pressure load by imposing a uniform stress (pressure) field [20–22,25,29,30]. In the velocity control approach, the normalization condition is obtained by simulating the action of pressure load with a uniform velocity field [23–24,26–28]. Particularly, in the finite-element limit analysis of circular hollow cylinders under internal pressure [26–28], we adopted the velocity (or displacement) control approach with the innermost edge expanded uniformly at a constant speed in the radial direction. It is noted that all the previous work [8,20–30] were conducted numerically by using a combined smoothing and successive approximation (CSSA) algorithm presented by Yang [33]. Particularly, the author and his co-worker extended the CSSA algorithm [33] with rigorous convergence analysis and validation to sequential limit analysis of viscoplasticity problems [26], or/and involving materials with nonlinear isotropic hardening [27–29].

The paper is aimed to analytically and numerically investigate the interesting interaction of strengthening and weakening behavior of pressurized cylinders made of strain-hardening viscoplastic materials. By the concept of sequential limit analysis, the plastic limit loads are acquired by solving a sequence of limit analysis problems via computational optimization techniques based on the CSSA algorithm [33]. Meanwhile, the velocity control is employed as a computational strategy to simulate the action of pressure. The resulting onset of instability and the stability condition corresponding to the velocity control are firstly investigated analytically in the paper to fully reveal the strength-

ing and weakening interaction. It is also noted that the Norton-Hoff viscoplastic model is utilized in the previous work [26,28] to consider the strain-rate sensitivity as utilized in regularized limit analysis [34]. On the other hand, the current work involving the strain-rate sensitivity is based on the rigid-plastic model with the updating yield strength step-wisely.

2. Problem formulation

We consider a plane-strain viscoplastic problem of the von Mises-type material with nonlinear isotropic hardening. It is noted that such problems feature in involving hardening material properties and weakening behavior corresponding to the strain-rate sensitivity in addition to widening deformation. The purpose is to seek the plastic limit load of a pressurized thick-walled hollow cylinder. Naturally, the problem statement leads to the lower bound formulation. By employing duality theorems [e.g. 8,13], we can establish the corresponding upper bound formulation from the lower bound formulation and further theoretically equates the greatest lower bound to the least upper bound. Therefore, we can approach the real limit solution by maximizing the lower bound or by minimizing the upper bound.

2.1. Problem statement (lower bound formulation)

We consider a general plane-strain problem with the domain D consisting of the static boundary ∂D_s and the kinematic boundary

∂D_k [13]. The quasi-static problem is to seek the maximum allowable driving load under constraints of static and constitutive admissibility such that

$$\begin{aligned} &\text{maximize } q(\sigma) \\ &\text{subject to } \nabla \cdot \sigma = 0 \quad \text{in } D \\ &\quad \sigma \cdot \bar{n} = q \bar{t} \quad \text{on } \partial D_s \\ &\quad \|\sigma\|_{\vee} \leq \sigma_Y \quad \text{in } D \end{aligned} \tag{1}$$

where \bar{n} indicates the unit outward normal vector of the boundary and the traction vector \bar{t} is scalable distribution of the driving load on ∂D_s with the load factor q ; $\|\sigma\|_{\vee}$ means the von Mises primal norm on stress tensor σ and σ_Y is a material constant denoting the yield strength. Therefore, this constrained problem is to maximize the load factor q representing the magnitude of the driving load for each step.

The primal problem (1) is the lower bound formulation seeking the maximum solution under constraints of static and constitutive admissibility. The statically admissible solutions satisfy the equilibrium equation and the static boundary condition. And the constitutive admissibility is stated by the yield criterion in an inequality form. We can interpret the solutions as sets as shown in the work of Huh and Yang [8], Yang [30]. First, the equilibrium equation is linear and the constitutive inequality is convex and bounded. Accordingly, the intersection of statically admissible set and constitutively admissible set is convex and bounded. Moreover, the existence of a unique maximum to the convex programming problem is confirmed.

2.2. Upper bound formulation

Now we intend to transform the lower bound formulation to the upper bound formulation by firstly restating weakly equilibrium equations in the form as

$$\int_D \bar{u} \cdot (\nabla \cdot \sigma) dA = 0 \tag{2}$$

where \bar{u} is a kinematically admissible velocity field. Integrating by parts, using the divergence theorem and imposing static boundary conditions, we may rewrite Eq. (2) to give an expression for $q(\sigma)$ as

$$\begin{aligned} \int_{\partial D_s} \bar{u} \cdot q \bar{t} dS &= q \int_{\partial D_s} \bar{u} \cdot \bar{t} dS \\ &= \int_D \sigma : \dot{\epsilon} dA \end{aligned} \tag{3}$$

where $\dot{\epsilon}$ is the strain-rate tensor.

Since the power $\sigma : \dot{\epsilon}$ is nonnegative. It is clear that $\sigma : \dot{\epsilon} = |\sigma : \dot{\epsilon}|$. Further, according to a generalized Hölder inequality [35], and the normality condition in plasticity [36], it results in

$$\sigma : \dot{\epsilon} = |\sigma : \dot{\epsilon}| \leq \|\sigma\|_{\vee} \|\dot{\epsilon}\|_{-\vee} = \bar{\sigma} \dot{\bar{\epsilon}} \tag{4}$$

where $\|\dot{\epsilon}\|_{-\vee}$ is the dual norm [8] of $\|\sigma\|_{\vee}$ based on the flow rule associated with the von Mises yield criterion. $\bar{\sigma}$ is the equivalent stress and $\dot{\bar{\epsilon}}$ is the equivalent strain.

Combining Eqs. (3) and (4) and considering the constitutive law $\|\sigma\|_{\vee} \leq \sigma_Y$, we have

$$\begin{aligned} q \int_{\partial D_s} \bar{u} \cdot \bar{t} dS &= \int_D \sigma : \dot{\epsilon} dA \leq \int_D \|\sigma\|_{\vee} \|\dot{\epsilon}\|_{-\vee} dA \\ &\leq \sigma_Y \int_D \|\dot{\epsilon}\|_{-\vee} dA \end{aligned} \tag{5}$$

To further deal with the left-hand side of the inequality (5), we can adopt the velocity control along the innermost boundary as a computational strategy, namely a normalization condition in the computations. By using the velocity control, the velocity field \bar{u}

along the boundary ∂D_s is prescribed as \bar{u}_s in each step. Therefore, we have

$$\int_{\partial D_s} \bar{u} \cdot \bar{t} dS = G(\bar{u}_s, S) \tag{6}$$

where $G(\bar{u}_s, S)$ is a constant in each step but may be of various values in a process. Therefore, $q(\sigma)$ can be bounded above by $\bar{q}(\bar{u})$ as

$$q(\sigma) \leq \frac{\sigma_Y}{G} \int_D \|\dot{\epsilon}\|_{-\vee} dA = \bar{q}(\bar{u}) \tag{7}$$

Thus, the upper bound formulation is stated in the form of a constrained minimization problem as

$$\begin{aligned} &\text{minimize } \bar{q}(\bar{u}) \\ &\text{subject to } \bar{q}(\bar{u}) = \frac{\sigma_Y}{G} \int_D \|\dot{\epsilon}\|_{-\vee} dA \\ &\nabla \cdot \bar{u} = 0 \quad \text{in } D \\ &\text{kinematic boundary conditions on } \partial D_k \end{aligned} \tag{8}$$

Therefore, the upper bound formulation seeks sequentially the least upper bound on kinematically admissible solutions. Accordingly, the primal-dual problems (1) and (8) are convex programming problems following the work of Huh and Yang [8] and as shown by Yang [13]. Thus, there exist a unique maximum and minimum to problems (1) and (8), respectively.

Thus, the extreme values of the lower bound functional $q(\sigma)$ and its corresponding upper bound functional $\bar{q}(\bar{u})$ are equal to the unique, exact solution q^* for each step in a process. Namely

$$\text{maximize } q(\sigma) = q^* = \text{minimize } \bar{q}(\bar{u}) \tag{9}$$

3. Computations

Traditionally, the assumption of a suitable failure mechanism [37] is critical to reduce the duality gap between the lower bound and the upper bound. However, finite-element limit analysis can be applied effectively to more complex problems by the use of finite-element methods [16] together with mathematical programming techniques [17].

By sequential limit analysis, the pressurized problem is formulated as a sequence of limit analysis problems and solved iteratively by a combined smoothing and successively approximation (CSSA) algorithm [33]. The CSSA algorithm adopted is comparable for its simple implementation and unconditional convergence. Upper bound plastic limit loads are then to be acquired iteratively through a computational optimization procedure.

3.1. Discretized functional

The upper bound formulation turns out to a constrained quadratic programming problem. The constrained minimization problem (8) is then stated approximately in the finite-element discretized form such that

$$\begin{aligned} &\text{minimize } \bar{q}(\{U\}) = \sum_{e=1}^{N_e} \frac{\sigma_Y}{G} \sqrt{\{U\}^t [K_{e1}] \{U\}} \\ &\text{subject to } \{U\}^t \{C\} = 0 \end{aligned} \tag{10}$$

where N_e denotes the number of elements used to discretize the domain; $[K_{e1}]$ is the element stiffness matrix; $\{U\}$ is the nodal-point velocity vector and superscript t denotes transposition and $\{C\}$ is a coefficient matrix.

3.2. Numerical algorithm

The CSSA algorithm presented by Yang [33] is now utilized to deal with the nonlinear problem (10) sequentially. Accordingly, the functional at the current step n is reorganized in the following form:

$$\begin{aligned} & \text{minimize } \tilde{q}(\{U\}) + \frac{\beta}{2} p(\{U\}) \\ & \text{with } p(\{U\}) = \sum_{e=1}^{N_e} \{U\}^t [K_{e2}] \{U\} \end{aligned} \quad (11)$$

where the penalty parameter β is a sufficiently large positive constant [38], and $[K_{e2}]$ is the element stiffness matrix.

In the paper, the behavior of viscoplastic, nonlinear isotropic hardening is described in the form as [39]

$$\sigma_Y = [\sigma_\infty - (\sigma_\infty - \sigma_0) \exp(-h\bar{\varepsilon})] \left(\frac{\dot{\bar{\varepsilon}}}{\dot{\bar{\varepsilon}}_0} \right)^m \quad (12)$$

where σ_0 is the initial yield strength, σ_∞ is the saturation value of σ_0 and h is the hardening exponent. $\bar{\varepsilon}$ is the equivalent strain and $\dot{\bar{\varepsilon}}$ the equivalent strain rate. $\dot{\bar{\varepsilon}}_0$ and m are positive-valued material parameters called the reference strain rate and strain-rate sensitivity, respectively.

While conducting a sequence of limit analysis problems sequentially, we need to update the current yield criterion in addition to the configuration of the deforming structures. At the first step, we have the equivalent strain $\bar{\varepsilon}^1 = 0$. For the current step $n \geq 2$, the value of $\bar{\varepsilon}^n$ is obtained as the following expression:

$$\bar{\varepsilon}^n = \sum_{i=1}^{n-1} \dot{\varepsilon}_i \Delta t_i \quad (13)$$

where Δt_i is the step size.

Further, we update the yield strength in the form as

$$(\sigma_Y)_{j+1}^n = [\sigma_\infty - (\sigma_\infty - \sigma_0) \exp(-h\bar{\varepsilon}^n)] \left(\frac{\dot{\varepsilon}_{j+1}^n}{\dot{\varepsilon}_0} \right)^m \quad (14)$$

where $(\sigma_Y)_{j+1}^n$ is the yield strength updated for the current iteration ($j+1$) of the n th step, $\dot{\varepsilon}_{j+1}^n$ is the equivalent strain rate updated in the ($i+1$)th iteration of the n th step with the current velocity vector $\{U\}_{j+1}$.

To solve the minimization problem (11), we apply the necessary condition for the minimum of $\tilde{q}(\{U\}) + (\beta/2)p(\{U\})$, namely taking its first derivative with respect to $\{U\}$. Moreover, the objective functional is smoothed by a small real number δ to overcome the numerical difficulty resulting from non-smoothness over some rigid regions [8,29]. Reorganizing the nonlinear equations, linear matrix–vector equations are then produced as

$$[K]\{U\} = 0 \quad (15)$$

with

$$[K]\{U\} = \sum_{e=1}^{N_e} (\bar{\sigma})_{j+1}^n \frac{[K_{e1}]\{U\}_{j+1}}{\sqrt{\{U^*\}_j^t [K_{e1}]\{U^*\}_j + \delta^2}} + \beta \sum_{e=1}^{N_e} [K_{e2}]\{U\}_{j+1} \quad (16)$$

where the subscriptions $j, (j+1)$ indicate quantities corresponding to any successive iterations. In Eq. (16), $\{U\}_{j+1}$ is the unknown at the current iteration ($j+1$) with $\{U^*\}_j$ calculated at the preceding iteration j . For the case $j = 0$, an arbitrary $\{U\}_0$ is adopted to start the iterations. A monotonically convergent sequence of $\tilde{q}(\{U^*\}_j)$ is then generated iteratively. Stopping criterion based on the ratio of Euclidean norms $E_u = \|\{U^*\}_j - \{U^*\}_{j-1}\|_2 / \|\{U^*\}_{j-1}\|_2$ is applied to check the convergence of each step. All the abovementioned procedures have been summarized as a flowchart shown in the previous work by Leu and Chen [29].

4. Analytical solutions

For rigorous validation, we derive the analytical solutions of thick-walled hollow cylinders made of strain-hardening viscoplastic materials subjected to internal pressure in plane-strain conditions. In addition to the plastic limit load, it is also interesting to show the interaction between strengthening and weakening behavior during the deformation process. Therefore, the onset of instability and the stability condition are also derived analytically for rigorous validation. Note that the hardening exponent $h = \sqrt{3}$ is used in the derivations. And the boundary conditions $\sigma_r(r = a) = P_i$, $\sigma_r(r = b) = 0$ are considered.

4.1. Plastic limit load

We consider a plane-strain problem involving a thick-walled hollow cylinder with the initial interior and exterior radii denoted by a_0 and b_0 . Also, its current interior and exterior radii are denoted by a and b . The cylinder concerned is made of strain-hardening viscoplastic materials simulated by the von Mises model. The behavior of viscoplastic, nonlinear isotropic hardening is as adopted by Haghi and Anand [39] as shown in Eq. (12).

As detailed in the previous work [28], we can obtain the plastic limit load expressed in the form as

$$\begin{aligned} \frac{P_i}{\sigma_0} = & \left(\frac{1}{\sqrt{3}} \right)^{m+1} \left(\frac{2\dot{a}a}{\dot{\varepsilon}_0} \right)^m \left[\frac{1}{m} \left(\frac{1}{b^{2m}} - \frac{1}{a^{2m}} \right) \right. \\ & \left. + \frac{1}{m+1} \left(\frac{\sigma_\infty}{\sigma_0} - 1 \right) (a_0^2 - a^2) \left(\frac{1}{a^{2m+2}} - \frac{1}{b^{2m+2}} \right) \right] \end{aligned} \quad (17)$$

where \dot{a} is the current velocity of the interior radius. Note that, the sign convention for the internal pressure P_i is positive for tension and negative for compression.

For the case with $m = 0$

$$\lim_{m \rightarrow 0} \frac{a^{-m} - a^m b^{-2m}}{m} = \ln \left(\frac{b^2}{a^2} \right) \quad (18)$$

Thus, we reduce the viscoplasticity problems to rate independent plasticity problems [27] with the strain-rate sensitivity $m = 0$, such that

$$\frac{P_i}{\sigma_0} = \frac{1}{\sqrt{3}} \left[\ln \left(\frac{a^2}{b^2} \right) + \left(\frac{\sigma_\infty}{\sigma_0} - 1 \right) \left(\frac{a_0^2}{a^2} - \frac{b_0^2}{b^2} \right) \right] \quad (19)$$

For the case with $\sigma_\infty = \sigma_0$, we reduce to non-hardening power-law viscoplasticity problems such that

$$\frac{P_i}{\sigma_0} = \frac{1}{m} \left(\frac{1}{\sqrt{3}} \right)^{m+1} \left(\frac{2\dot{a}a}{\dot{\varepsilon}_0} \right)^m \left[\left(\frac{1}{b^{2m}} - \frac{1}{a^{2m}} \right) \right] \quad (20)$$

It is also noted that such analytical solution for non-hardening power-law viscoplasticity problems is available with the concept for the first-step limit values in the literature as presented by Peirce et al. [40].

4.2. Onset of instability

For the pressurized problem involving strain-hardening viscoplastic materials, there is an instability phenomenon during the whole deformation process. Namely, the instability is about the occurrence of a weakening phenomenon while the effect of strain-rate sensitivity and widening deformation counteracts that of the strain hardening [31,32]. Therefore, investigation of the onset of instability is to consider the existence of the maximum value of the limit load. We apply the necessary condition for the maximum

of P_i/σ_0 , namely the following mathematical expression

$$\frac{\partial(P_i/\sigma_0)}{\partial a} = 0 \tag{21}$$

Note that, the current interior radius is a and the value of \dot{a} is a constant for the velocity control. Thus, we obtain the onset of instability associated with the velocity control as in the form

$$\begin{aligned} &\frac{1}{a^{m+1}} + \frac{a^{m-1}}{b^{2m}} - \frac{2a^{m+1}}{b^{2m+2}} - \frac{\sigma_\infty/\sigma_0 - 1}{m+1} \left(\frac{2}{a^{m+1}} - \frac{2a^{m+1}}{b^{2m+2}} \right) \\ &- \frac{m+2}{m+1} (\sigma_\infty/\sigma_0 - 1) \frac{a_0^2 - a^2}{a^{m+3}} - \frac{m}{m+1} (\sigma_\infty/\sigma_0 - 1) \\ &\times \frac{a_0^2 - a^2}{b^{2m+2}} a^{m-1} + 2(\sigma_\infty/\sigma_0 - 1) \frac{a_0^2 - a^2}{b^{2m+4}} a^{m+1} = 0 \end{aligned} \tag{22}$$

Further, with the incompressibility condition $a^2 - a_0^2 = b^2 - b_0^2$, the nonlinear equation can be reorganized as

$$\begin{aligned} &(m+2)(\sigma_\infty/\sigma_0 - 1) \frac{a_0^2}{a^2} = (m\sigma_\infty/\sigma_0 + 1) \\ &- 2(m\sigma_\infty/\sigma_0 + 1) \frac{a^{2m+2}}{b^{2m+2}} + (m\sigma_\infty/\sigma_0 + 1) \frac{a^{2m}}{b^{2m}} \\ &- m(\sigma_\infty/\sigma_0 - 1) \frac{a^{2m} b_0^2}{b^{2m+2}} + 2(m+1)(\sigma_\infty/\sigma_0 - 1) \frac{a^{2m+2} b_0^2}{b^{2m+4}} \end{aligned} \tag{23}$$

To solve the nonlinear equation, we apply the method of fixed point iteration [41] to numerically acquire the onset of instability in terms of a/a_0 . Thus, the nonlinear equation is reorganized as

$$\begin{aligned} \frac{a_0^2}{a^2} = &\frac{1}{m+2} \frac{m\sigma_\infty/\sigma_0 + 1}{\sigma_\infty/\sigma_0 - 1} - \frac{2}{m+2} \frac{m\sigma_\infty/\sigma_0 + 1}{\sigma_\infty/\sigma_0 - 1} \frac{a^{2m+2}}{b^{2m+2}} \\ &+ \frac{1}{m+2} \frac{m\sigma_\infty/\sigma_0 + 1}{\sigma_\infty/\sigma_0 - 1} \frac{a^{2m}}{b^{2m}} - \frac{m}{m+2} \frac{a^{2m} b_0^2}{b^{2m+2}} \\ &+ 2 \frac{m+1}{m+2} \frac{a^{2m+2} b_0^2}{b^{2m+4}} \end{aligned} \tag{24}$$

And we get the solution of a/a_0 in the form ready for the method of fixed point iteration [41]

$$\frac{a}{a_0} = \left(\frac{1}{m+2} \frac{m\sigma_\infty/\sigma_0 + 1}{\sigma_\infty/\sigma_0 - 1} - \frac{2}{m+2} \frac{m\sigma_\infty/\sigma_0 + 1}{\sigma_\infty/\sigma_0 - 1} \frac{a^{2m+2}}{b^{2m+2}} + \frac{1}{m+2} \frac{m\sigma_\infty/\sigma_0 + 1}{\sigma_\infty/\sigma_0 - 1} \frac{a^{2m}}{b^{2m}} - \frac{m}{m+2} \frac{a^{2m} b_0^2}{b^{2m+2}} + 2 \frac{m+1}{m+2} \frac{a^{2m+2} b_0^2}{b^{2m+4}} \right)^{-1/2} \tag{25}$$

4.3. Stability condition

We come to consider the condition of stability, namely the existence of a hardening phenomenon before the weakening behavior. Mathematically, it is to consider the increase of the plastic limit load during the widening process expressed in the following form with the current interior radius a :

$$\frac{\partial(P_i/\sigma_0)}{\partial a} > 0 \tag{26}$$

Note that, the sign convention for the internal pressure P_i is positive for tension and negative for compression. Therefore, we have the following expression:

$$\begin{aligned} &\frac{1}{a^{m+1}} + \frac{a^{m-1}}{b^{2m}} - \frac{2a^{m+1}}{b^{2m+2}} - \frac{\sigma_\infty/\sigma_0 - 1}{m+1} \left(\frac{2}{a^{m+1}} - \frac{2a^{m+1}}{b^{2m+2}} \right) \\ &- \frac{m+2}{m+1} (\sigma_\infty/\sigma_0 - 1) \frac{a_0^2 - a^2}{a^{m+3}} - \frac{m}{m+1} (\sigma_\infty/\sigma_0 - 1) \\ &\times \frac{a_0^2 - a^2}{b^{2m+2}} a^{m-1} + 2(\sigma_\infty/\sigma_0 - 1) \frac{a_0^2 - a^2}{b^{2m+4}} a^{m+1} < 0 \end{aligned} \tag{27}$$

Certainly, the larger the value of σ_∞/σ_0 the more obvious the strengthening range. Therefore, the critical case of $a = a_0$ and $b = b_0$ is corresponding to the minimum value of σ_∞/σ_0 . Thus, corresponding to the viscoplastic strain-hardening behavior with the hardening exponent $h = \sqrt{3}$, we can substitute the values of $a = a_0$ and $b = b_0$ into the inequality (27) and get the existence of the stability condition as

$$\frac{\sigma_\infty/\sigma_0 - 1}{m+1} \left(\frac{2}{a_0^{m+1}} - \frac{2a_0^{m+1}}{b_0^{2m+2}} \right) > \frac{1}{a_0^{m+1}} + \frac{a_0^{m-1}}{b_0^{2m}} - \frac{2a_0^{m+1}}{b_0^{2m+2}} \tag{28}$$

After reorganization, we get the stability condition in terms of the yield strength ratio in the form as

$$\sigma_\infty/\sigma_0 > \frac{m+3}{2} + \frac{m+1}{2} \frac{(b_0/a_0)^2 - 1}{(b_0/a_0)^{2m+2} - 1} \tag{29}$$

For the case with the strain-rate sensitivity $m = 0$, we then obtain the stability condition reduced to the form as

$$\sigma_\infty/\sigma_0 > \frac{3}{2} + \frac{1}{2} = 2 \tag{30}$$

5. Comparisons and validations

We consider thick-walled cylinders made of strain-hardening viscoplastic materials subjected to internal pressure in plane-strain conditions. Comparisons between numerical results and analytical solutions are made to demonstrate the reliable applications of the computational optimization procedure presented in the paper.

The initial inner and outer radii of the hollow cylinder are denoted as a_0 and b_0 , respectively. The innermost edge is subjected to the action of internal pressure simulated by using the velocity control. The pressure needed to keep the expanding cylinder fully plastic is then computed sequentially by using the CSSA algorithm [33]. In the following case studies, we adopt the dimensional consistently parameters: $a_0 = 5.0$, $b_0 = 10.0$, $h = \sqrt{3}$, $\dot{a} = 1.0$, $\dot{\epsilon} = 1.0$, and a constant step size $\Delta t = 0.01$.

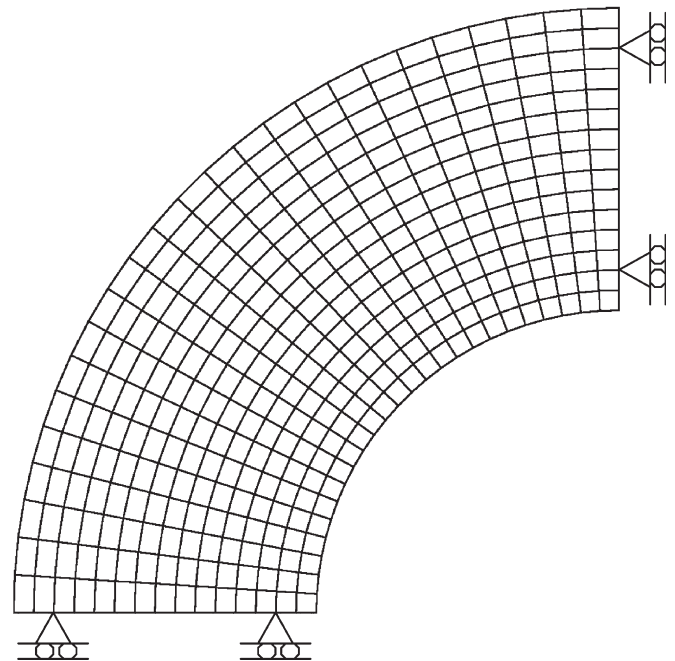


Fig. 1. Finite-element model of a thick-walled hollow cylinder.

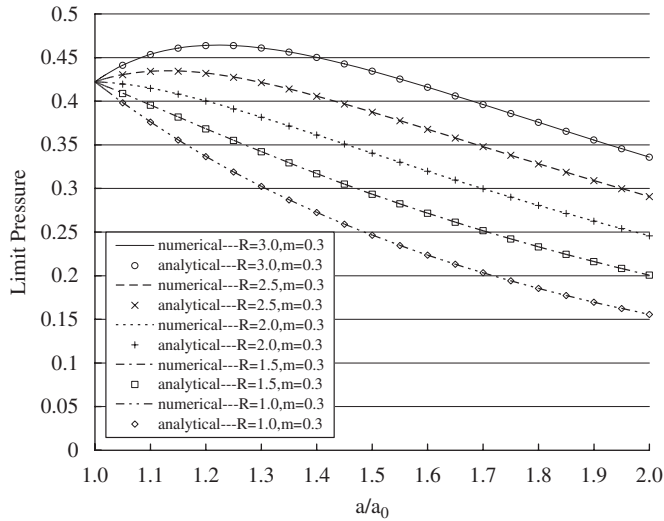


Fig. 2. Limit internal pressure (P_i/σ_0) versus the inner radius (a/a_0) with various yield strength ratios ($R = \sigma_\infty/\sigma_0$) and the strain-rate sensitivity $m = 0.3$.

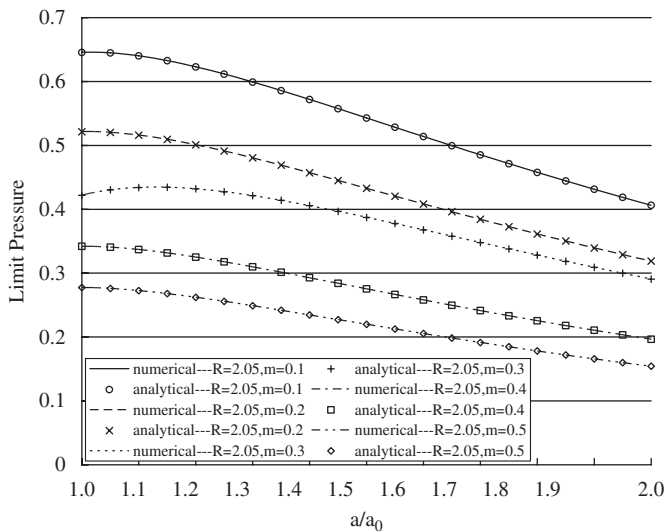


Fig. 3. Effect of the strain-rate sensitivity m on limit internal pressure (P_i/σ_0) with $R = \sigma_\infty/\sigma_0 = 2.05$.

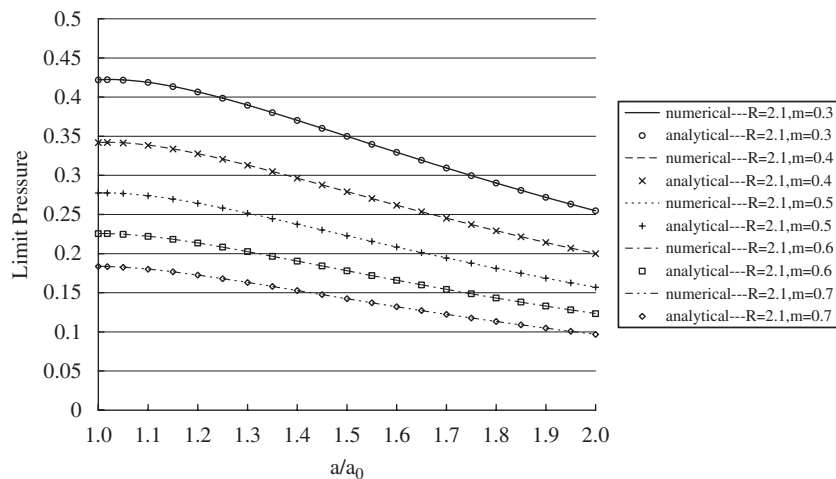


Fig. 4. Effect of the strain-rate sensitivity m on limit internal pressure (P_i/σ_0) with $R = \sigma_\infty/\sigma_0 = 2.1$.

Due to the loading and geometric symmetry, only one quarter of the axisymmetric structure is simulated for the circular hollow cylinder as shown in Fig. 1. With symmetry boundary conditions imposed along boundaries in the Cartesian coordinate system, one quarter of a cylinder is used to simulate axial symmetry. Four-node quadrilateral isoparametric elements are utilized to discretize the problem domain. A sequence of limit analysis problems is solved to obtain sequentially numerical solutions of deforming problems. Note that the first-step solution is the limit value of internal pressure causing the cylinder of dimensions a_0 and b_0 fully plastic. Following the first step, each step in sequential limit analysis starts with the result obtained in the preceding step to update the yield strength and geometry with the constant step size $\Delta t = 0.01$.

Numerical cases are considered with various values of the yield strength ratio, namely the hardening parameter, $R = \sigma_\infty/\sigma_0$ and the strain-rate sensitivity $m = 0.3$. With an arbitrarily initial value $\{U\}_0$ and the convergence tolerance $E_U = 1.0 E-5$, the results related to various values of the yield strength ratio $R = \sigma_\infty/\sigma_0 = 2.05$, $R = \sigma_\infty/\sigma_0 = 2.1$, $R = \sigma_\infty/\sigma_0 = 2.3$, respectively. As shown, all the computed upper bounds agree very well with the analytical solutions. That also demonstrates the validation of the step-wisely rigid-plastic model for the strain-rate sensitivity.

Based on the concept of sequential limit analysis, the paper is aimed to deal with the widening problems featuring in hardening material properties and weakening behavior. After the validation of the accuracy of the computational plastic limit load, the next issue is to demonstrate the interaction of the strengthening and weakening phenomenon. We concern the stability condition and the onset of the instability. Note that, the paper considers the viscoplastic strain-hardening behavior [39] with the hardening exponent $h = \sqrt{3}$. As detailed in analytical derivations, there exists strengthening phenomenon for $\sigma_\infty/\sigma_0 > (m + 3)/2 + ((m + 1)/2)((b_0/a_0)^2 - 1)/((b_0/a_0)^{2m+2} - 1)$ with the action of internal pressure simulated by the velocity control. Namely, the hollow cylinders with $\sigma_\infty/\sigma_0 > (m + 3)/2 + ((m + 1)/2)((b_0/a_0)^2 - 1)/((b_0/a_0)^{2m+2} - 1)$ are strengthened up until the onset of instability with the strain-hardening exponent $h = \sqrt{3}$. Following that, however, the weakening phenomenon is observed while the effect of the

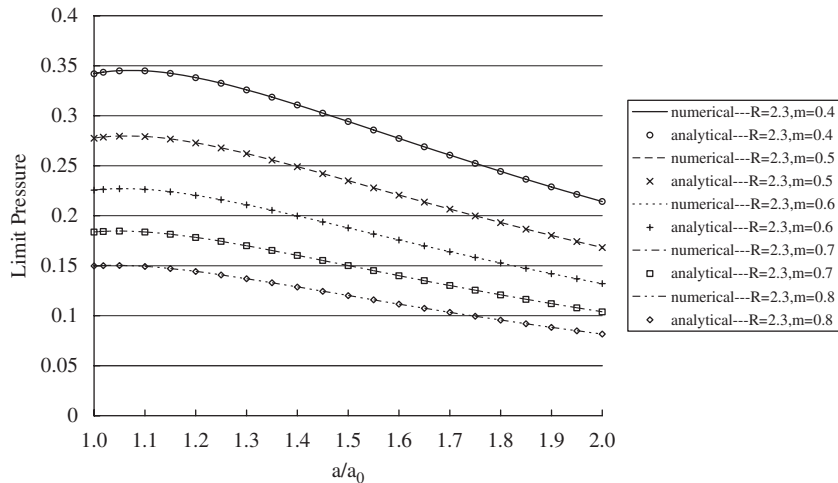


Fig. 5. Effect of the strain-rate sensitivity m on limit internal pressure (P_i/σ_0) with $R = \sigma_\infty/\sigma_0 = 2.3$.

Table 1

Effects of the yield strength ratio σ_∞/σ_0 and the strain-rate sensitivity m on the onset of instability in terms of the inner radius a/a_0

σ_∞/σ_0	m								
	0.1	0.2	0.3	0.4	0.5	0.6	0.7	0.8	
2.05	1.015	1.010	1.005	-	-	-	-	-	
2.1	1.033	1.028	1.022	1.015	1.009	1.002	-	-	
2.3	1.096	1.088	1.080	1.072	1.064	1.056	1.048	1.039	

Table 2

Effects of the strain-rate sensitivity m on the stability condition in terms of the yield strength ratio σ_∞/σ_0

m	σ_∞/σ_0								
	0.1	0.2	0.3	0.4	0.5	0.6	0.7	0.8	
2.009	2.021	2.035	2.052	2.071	2.093	2.117	2.143		

strain-hardening is counteracted by that of the strain-rate sensitivity m together with widening deformation.

As shown in Fig. 2, the strengthening phenomenon is more significant with a higher value of the hardening parameter in terms of the yield strength ratio $R = \sigma_\infty/\sigma_0$. On the other hand, the weakening behavior is corresponding to the strain-rate sensitivity m and widening deformation as shown in Figs. 3–4. Fig. 3 shows that there are significant strengthening phenomena for the cases with $R = \sigma_\infty/\sigma_0 = 2.05$, and $m = 0.1, 0.2$ and 0.3 , respectively. But there are no strengthening phenomena for the cases with $R = \sigma_\infty/\sigma_0 = 2.05$, and $m = 0.4$ and 0.5 , respectively. Fig. 4 illustrates that there is still a strengthening phenomenon even for the cases with $R = \sigma_\infty/\sigma_0 = 2.1$ and $m = 0.6$. But there is no obvious strengthening phenomenon for the case with $R = \sigma_\infty/\sigma_0 = 2.1$ and $m = 0.7$. However, the strengthening effect is dominant even for the case with $R = \sigma_\infty/\sigma_0 = 2.3$ and $m = 0.8$ as shown in Fig. 5.

Table 1 lists the analytical results by Eq. (25) showing the effects of the yield strength ratio $R = \sigma_\infty/\sigma_0$ and the strain-rate sensitivity m on the onset of instability in terms of inner radius a/a_0 . Table 2 lists the analytical results by the inequality (29) showing the effects of the strain-rate sensitivity m on the stability

condition in terms of the yield strength ratio $R = \sigma_\infty/\sigma_0$ with the ratio of the initial exterior radius to interior radius $b_0/a_0 = 2$. Again, the computed results and the analytical solutions for the onset of instability and the stability condition, respectively, agree very well as shown in Figs. 2–5.

6. Conclusions

The paper has systematically presented the numerical and analytical investigation of limit analysis of thick-walled cylinders under internal pressure made of strain-hardening viscoplastic materials [39]. As pointed out in the paper, it is also an interesting problem to demonstrate the interaction of strengthening and weakening behavior resulting from the properties of the strain-hardening and the strain-rate sensitivity during the deformation process.

By using the concept of sequential limit analysis, the plastic limit loads for plane-strain circular cylinders under internal pressure were acquired by solving a sequence of limit analysis problems via computational optimization techniques using a combined smoothing and successively approximation (CSSA) algorithm [33]. Numerically, the velocity control was adopted to simulate the action of internal pressure by a uniform velocity field along the innermost edge.

Based on the velocity control approach, the stability condition for the pressurized thick-walled hollow cylinders is also obtained analytically as $\sigma_\infty/\sigma_0 > (m + 3)/2 + ((m + 1)/2)((b_0/a_0)^2 - 1)/((b_0/a_0)^{2m+2} - 1)$ with the yield strength ratios σ_∞/σ_0 , the strain-rate sensitivity m , the hardening exponent $h = \sqrt{3}$, and the initial interior and exterior radii a_0 and b_0 . Namely, it is found that, with the hardening exponent $h = \sqrt{3}$, the strengthening phenomena exist only for the cases that the relationship $\sigma_\infty/\sigma_0 > ((m + 3)/(2)) + ((m + 1)/(2))(((b_0/a_0)^2 - 1)/((b_0/a_0)^{2m+2} - 1))$ is held between the strain-rate sensitivity m and the yield strength ratio σ_∞/σ_0 . On the other hand, the related onset of instability was obtained in an implicit form and solved in a novel way by the fixed point iteration [41].

Finally, validation of the present investigation is confirmed by good agreement between the analytical solutions and numerical results of the plastic limit load, the onset of instability and the stability condition.

Acknowledgments

Financial support from the National Science Council under Grant no. NSC 96-2221-E-157-003 for China Institute of Technology is gratefully acknowledged.

References

- [1] Anderheggen E, Knöpfel H. Finite element limit analysis using linear programming. *Int J Solids Struct* 1972;8(12):1413–31.
- [2] Bottero A, Negre R, Pastor J, Turgeman S. Finite element method and limit analysis theory for soil mechanics problems. *Comput Meth Appl Mech Eng* 1980;22(1):131–49.
- [3] Capsoni A, Corradi L. A finite element formulation of the rigid-plastic limit analysis problem. *Int J Num Meth Eng* 1997;40(11):2063–86.
- [4] Christiansen E. Computation of limit loads. *Int J Num Meth Eng* 1981;17(10):1547–70.
- [5] Corradi L, Luzzi L, Vena P. Finite element limit analysis of anisotropic structures. *Comput Meth Appl Mech Eng* 2006;195(41–43):5422–36.
- [6] Dang Hung N. Direct limit analysis via rigid-plastic finite elements. *Comput Meth Appl Mech Eng* 1976;8(1):81–116.
- [7] Hodge PG, Belytschko T. Numerical methods for the limit analysis of plates. *J Appl Mech ASME* 1968;35:796–802.
- [8] Huh H, Yang WH. A general algorithm for limit solutions of plane stress problems. *Int J Solids Struct* 1991;28(6):727–38.
- [9] Jiang GL. Nonlinear finite element formulation of kinematic limit analysis. *Int J Num Meth Eng* 1995;38(16):2775–807.
- [10] Li HX, Yu HS. Kinematic limit analysis of frictional materials using nonlinear programming. *Int J Solids Struct* 2005;42(14):4058–76.
- [11] Pastor J, Thai TH, Francescato P. New bounds for the height limit of a vertical slope. *Int J Numer Meth Anal Meth Geomech* 2000;24(2):165–82.
- [12] Sloan SW. Upper bound limit analysis using finite elements and linear programming. *Int J Numer Meth Anal Meth Geomech* 1989;13(3):263–82.
- [13] Yang WH. Admissibility of discontinuous solutions in mathematical models of plasticity. In: Yang WH, editor. *Topics in plasticity*. MI: AM Press; 1991. p. 241–60.
- [14] Yu HS, Sloan SW. Limit analysis of anisotropic soils using finite elements and linear programming. *Mech Res Commun* 1994;21(6):545–54.
- [15] Zhang YG, Zhang P, Xue WM. Limit analysis considering initial constant loadings and proportional loadings. *Comput Mech* 1994;14(3):229–34.
- [16] Reddy JN. *An introduction to the finite element method*. New York: McGraw-Hill; 1993.
- [17] Luenberger DG. *Linear and nonlinear programming*. MA: Addison-Wesley; 1984.
- [18] Corradi L, Panzeri N, Poggi C. Post-critical behavior of moderately thick axisymmetric shells: a sequential limit analysis approach. *Int J Struct Stab Dyn* 2001;1(3):293–311.
- [19] Corradi L, Panzeri N. A triangular finite element for sequential limit analysis of shells. *Adv Eng Software* 2004;35(10–11):633–43.
- [20] Huh H, Lee CH. Eulerian finite-element modeling of the extrusion process for work-hardening materials with the extended concept of limit analysis. *J Mater Process Tech* 1993;38(1–2):51–61.
- [21] Huh H, Lee CH, Yang WH. A general algorithm for plastic flow simulation by finite element limit analysis. *Int J Solids Struct* 1999;36(8):1193–207.
- [22] Huh H, Kim KP, Kim HS. Collapse simulation of tubular structures using a finite element limit analysis approach and shell elements. *Int J Mech Sci* 2001;43(9):2171–87.
- [23] Hwan CL. An upper bound finite element procedure for solving large plane strain deformation. *Int J Num Meth Eng* 1997;40(10):1909–22.
- [24] Hwan CL. Plane strain extrusion by sequential limit analysis. *Int J Mech Sci* 1997;39(7):807–17.
- [25] Kim KP, Huh H. Dynamic limit analysis formulation for impact simulation of structural members. *Int J Solids Struct* 2006;43(21):6488–501.
- [26] Leu SY. Limit analysis of viscoplastic flows using an extended general algorithm sequentially: convergence analysis and validation. *Comput Mech* 2003;30(5–6):421–7.
- [27] Leu SY. Convergence analysis and validation of sequential limit analysis of plane-strain problems of the von Mises model with nonlinear isotropic hardening. *Int J Num Meth Eng* 2005;64(3):322–34.
- [28] Leu SY. Analytical and numerical investigation of strain-hardening viscoplastic thick-walled cylinders under internal pressure by using sequential limit analysis. *Comput Meth Appl Mech Eng* 2007;196(25–28):2713–22.
- [29] Leu SY, Chen JT. Sequential limit analysis of rotating hollow cylinders of nonlinear isotropic hardening. *CMES* 2006;14(2):129–40.
- [30] Yang WH. Large deformation of structures by sequential limit analysis. *Int J Solids Struct* 1993;30(7):1001–13.
- [31] Chakrabarty J. *Theory of plasticity*. New York: McGraw-Hill; 1987.
- [32] Rimrott FPJ. On the plastic behavior of rotating cylinders. *J Appl Mech ASME* 1960;27:309–15.
- [33] Yang WH. A variational principle and an algorithm for limit analysis of beams and plates. *Comput Meth Appl Mech Eng* 1982;33(1–3):575–82.
- [34] Jiang GL. Regularized method in limit analysis. *J Eng Mech* 1994;120(6):1179–97.
- [35] Yang WH. On generalized Hölder inequality. *Nonlinear Anal Theory Meth Appl* 1991;16:489–98.
- [36] Drucker DC. A definition of stable inelastic material in the mechanics of continua. *J Appl Mech ASME* 1959;81:101–6.
- [37] Chen WF. *Limit analysis and soil plasticity*. Amsterdam: Elsevier; 1975.
- [38] Reddy JN. *Applied functional analysis and variational methods in engineering*. New York: McGraw-Hill; 1986.
- [39] Hagh M, Anand L. Analysis of strain-hardening viscoplastic thick-walled sphere and cylinder under external pressure. *Int J Plast* 1991;7(3):123–40.
- [40] Peirce D, Shih CF, Needleman A. A tangent modulus method for rate dependent solids. *Comput Struct* 1984;18(5):875–87.
- [41] Ciarlet PG. *Introduction to numerical linear algebra and optimisation*. Cambridge: Cambridge University Press; 1989.